9th Asia-Pacific Conference on Wind Engineering
Auckland, New Zealand
3-7 December 2017

Numerical Simulation for Predicting Snow Accretion Distribution on Building Wall

Y. Tabata[1] and K. Otsuka[1]

[1]Technical Research Institute, Obayashi Corporation
Kiyose-Shi, Tokyo 204-8558, Japan

Abstract

A numerical model of snow particle transport was developed to predict snow adhesion on buildings. The equations of motion of snow particles in a Lagrangian formulation are employed to calculate the movement of snow particles in air flow fields, determine by CFD (Computational Fluid dynamics) calculations in order to appropriately take into account the effects of the inertia of snow. The model is applied to simulations of snow accretion on objects of different sizes, ranging from laboratory scale to real building scale. The results obtained from the simulation well reproduced the differences in snow accretion on small and large objects observed outside.

Introduction

There exist many kinds of snow-related problems in building construction in Japan because a number of snow-rich regions exist in Japan. Roof snow loads, snowdrifts around buildings, and adhesion or accumulation of snow on the outside walls of buildings are examples of such problems. In recent years, numerical approaches with CFD techniques have become useful tools in considering measures against these problems. CFD simulations were employed in previous studies on snowdrift on the ground surfaces around buildings (e.g.[1]–[2]).

The adhesion of snow to the outside walls of buildings can sometimes be problematic. Snow falling under the effect of gravity over certain vertical stretches can hit and damage objects existing below, such as glass roofs for example, and occasionally, pedestrians or vehicles. This can occur even if the falling snow or ice packs are not large in size and weight. However, the mechanisms of snow adhesion to building walls have many aspects yet to be understood.

Figure 1 shows instances of snow adhesion to a utility pole and a building wall observed during outdoor surveys on snowy days. Differences in the ways of adhesion are apparent. Snow adheres to the rim of the building wall, while it is concentrated around the center of the utility pole. These facts suggest that the manner of snow adhesion may depend on the sizes of the objects. Thus, in order to prevent accidents caused by falling snow pack from taking place, it is important to identify the parts of building walls where snow adhesion can occur.

(1) Snow adhesion on concrete utility pole (2) Snow adhesion on building wall

Figure 1. Examples of snow accretion observed outdoors.

The purpose of this study is to develop a numerical method to predict snow adhesion distribution on a building exterior. The first part of this paper describes the wind tunnel experiments carried out to investigate snow adhesion to the simple-shaped objects, that is, a flat plate, which is one type of building member frequently used for exterior walls. In the latter part of the paper, a numerical model based on the equations of motion of snow particles in a Lagrangian formulation is introduced. The results of some numerical experiments on the relationships between the patterns of snow adhesion and object sizes, which range from those in a laboratory to those in the real world, will be shown.

Wind Tunnel Experiments for Snow Accretion to Simple Cross Section

Outline of Wind Tunnel Experiment

In order to investigate snow adhesion to objects with simple cross sections, typical of members frequently used as vertical fins on building walls, a series of wind tunnel experiments were carried out at the Cryospheric Environment Simulator of the Snow and Ice Research Center of the National Research Institute for Earth Science and Disaster Prevention in Japan. Figure 2 shows an outline of the wind tunnel experiment. The wind tunnel had a cross section of 1.0 m × 1.0 m, and all the experiments were conducted by setting the air temperature at -3 ºC.

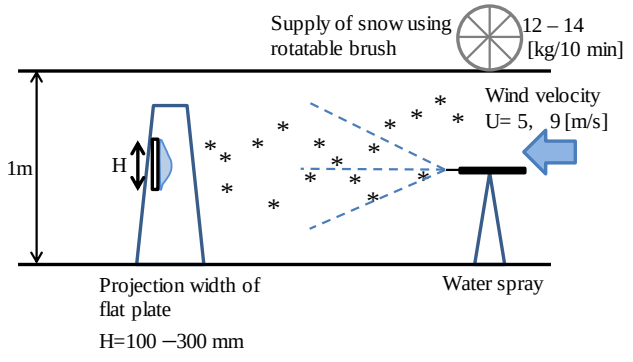

Figure 2. Outline of wind tunnel experiment.

Case No.	Projection width H [mm]	Wind Velocity u [m/s]	Experimental time [min]
Case1	100	9	30
Case2	200		30
Case3	300		30
Case4	100	5	30

Table 1. Test cases

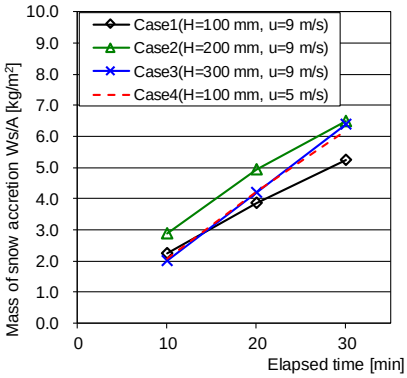

Figure 3. Mass of snow accretion per unit area.

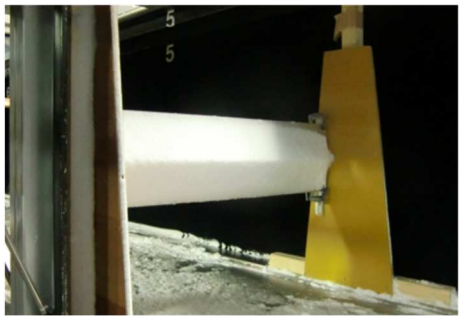

Figure 4. Example of snow accretion on flat plate for Case2 (H = 200 mm).

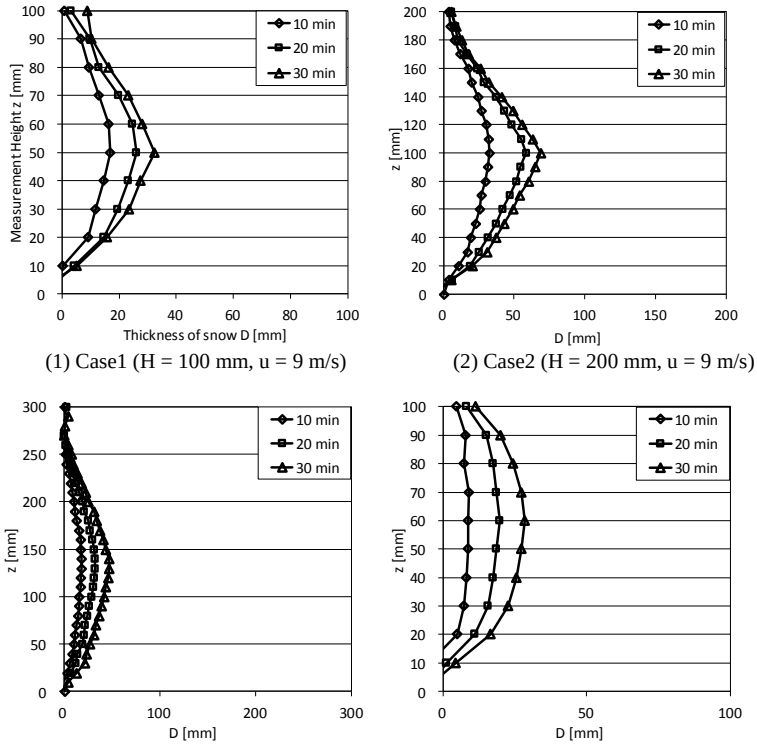

(1) Case1 (H = 100 mm, u = 9 m/s) (2) Case2 (H = 200 mm, u = 9 m/s)

(3) Case3 (H = 300 mm, u = 9 m/s) (4) Case4 (H = 100 mm, u = 5 m/s)

Figure 5. Temporal changes in cross section during snow accretion.

The seeding of artificial snow in the wind tunnel flow was done through a window in the ceiling of the wind tunnel at several meters upwind of the test section. In the experiment, in order to roughly approximate the adhesion of wet snow, fine water droplets are also seeded in the wind tunnel flow by using a water nozzle placed near the upwind end of the wind tunnel.

The cases conducted in the experiments are listed in Table 1. Three kinds of flat plates having different projection widths (H = 100, 200, and 300 mm) were used, with uniform flow velocities of U = 5 and 9 m/s. In the experiments, the lengths of time of the individual cases were generally set at 30 min. The thickness of the adhered snow was measured every 10 min using a laser displacement meter to see the development in time of snow adhesion. In addition, the mass flux of airborne snow particles in each case was measured by collecting snow particles using a netlike bag that was set at the same place as the test pieces.

Results of Wind Tunnel Experiment

Figure 3 shows temporal variations in the mass of the accreted snow pack on the flat plate per unit area. In all cases, the masses of the adhered snow almost linearly increased with time. However, the tendency of the growth rate slowed down slightly after 20 min passed from the start of the experiments, except in Case3. Figure 5 shows temporal changes of the shapes of the cross sections of snow in each case, and Figure 4 shows a photo of the snow pack adhered to the flat plate (Case2).

In all cases, the cross sections of snow pack at a time of 30 min have nearly triangular shapes with a central peak on the windward side, as shown in Figure 4. In Case1 and Case2 (H = 100, 200 mm, U = 9 m/s), the triangular nature of the cross sections already became clear when 20 min passed from the start of the experiment, and the rate of increase of the mass of the snow pack per unit time decreased with time because of a gradual shrinking of the stagnation region existing just in front of the test piece as the snow pack became triangular and grew in size. In Case3 (H = 300 mm), the rate of growth of the snow pack, which indicates the rate of increase of the maximum snow thickness here, was slower and held nearly constant over the period of the experiment, in contrast to Case1 and Case2.

One aspect of the influences of the wind velocities on the development of snow adhesion can be seen in the temporal evolution of the cross sections of the accreted snow pack in Case4 (H = 100 mm), as shown in Figure 5, where the experiment was done at a wind velocity of 5 m/s. The upwind surfaces of the snow pack are smoothly curved, and the growth rate of the snow pack is kept nearly constant. This indicates the snow accretion is still progressing at the time of 30 min. The maximum thickness of the snow pack in Case4 at 30 min is not significantly different from that in Case1 when the projection width of the test piece is the same as that in Case4 but the wind velocity was 9 m/s.

The mass of the accreted snow at the end of the experiments is, however, larger in Case4 than in Case1. This difference will be the results of the difference in the mass balances of snow between Case1 and Case4. Regarding this point, it is considered that the mass balance between the snow accretion owing to the collision of snow particles with the flat plate and erosion at the surface of the snow pack (whose rate depends significantly on the strength of the wind component tangent to the snow surface) will be achieved faster in Case1 than in Case4. Weaker tangential wind in Case4 at the surface of the snow pack, and therefore weaker erosion, may have resulted in the formation of the larger snow pack than that in Case1.

Prediction of Snow Accretion to Objects of Different Sizes

Outline of Computation

In order to better understand the processes responsible for making differences in the way of snow adhesion among objects having different projection areas to the wind direction as observed outdoor on snow days, a semi-empirical snow accretion model was developed for use in predicting snow adhesion to objects. The Lagrangian method was adopted to represent the

	Projection width W
Small objects (building material scale)	0.2, 0.5, 1.0 [m]
Middle scale	2, 5, 10 [m]
Large objects (building scale)	30, 60, 80 [m]

Table 2. Computational Cases

Projection area of snowflake S	50 [mm^2]
Mass of snowflake	$0.12S^{1.07}$
Drag coefficient C_D	0.85[-]

Table 3. Parameters of snow particles (Snowflake) [3]

Lateral and upper boundaries	free-slip
Ground surface boundary	z_0 type log law
Building surface boundary	Generalized log law for smooth wall
Inflow boundary	Uniform inflow
Outflow boundary	Method of characteristics
Convection terms	Third-order upwind scheme
Turbulence model	Durbin type k-ε model

Table 4. Computational Conditions

motion of snow particles in order for the effects of the inertia force to be readily taken into account. The equation of motion of a single snow particle is written as Equation (1).

$$m\frac{d\mathbf{V}}{dt} = -m\mathbf{g} - \frac{1}{2}\rho_{air} C_D A|\mathbf{V} - \mathbf{V}_{air}|(\mathbf{V} - \mathbf{V}_{air}) \quad (1)$$

V: particle velocity [m/s], $\boldsymbol{V_{air}}$*:* wind velocity [m/s], *m:* mass of a snow particle [kg], ρ_{air}: air density (=1.2) [kg/m^3], *A:* projection area of snow particle [m^2], C_D*:* drag coefficient [-].

A number of snow particles are numerically generated randomly at the inflow boundary, and their motions within the CFD-generated air flows are traced by numerically integrating equation (1) for fixed CFD-produced air flows. The ratios of the collision of snow particles to the objects placed in the flow fields are calculated. The ratio of collision is defined as the number of particles colliding with the object per unit time, divided by the number of particles passing through the area per unit time at an inflow boundary having the same projection area as the objects.

All test cases conducted in the computations are listed in Table2, and an example of the computational domain is illustrated in Figure 6. *x*, *y*, and *z* are the components of the spatial coordinates in the leeward, transverse, and vertical directions, respectively. The computational domains in individual cases have different sizes and grid resolutions depending on the sizes of the objects treated here, which is ranging from 0.1m to tens of meters in width with respect to the inflow winds. The physical properties of snow particles assumed in this study are listed in Table 3. In the simulations of this study, the physical properties of snow particles were given in reference to the properties of rimed snowflakes investigated by Ishizaka [3] during field measurements. With a uniform inflow wind speed of 10.0 [m/s] and the computational conditions given in Table 4, the ratios of the collision of snow particles are calculated.

Results and Discussion

Figure 7 shows comparisons of the airflow streamlines and the trajectories of snow particles around the objects in the horizontal plane at z/H = 0.7 (H: object height) for cases with projection widths of W = 80 m, 10 m, and 0.2 m obtained by CFD. In the case

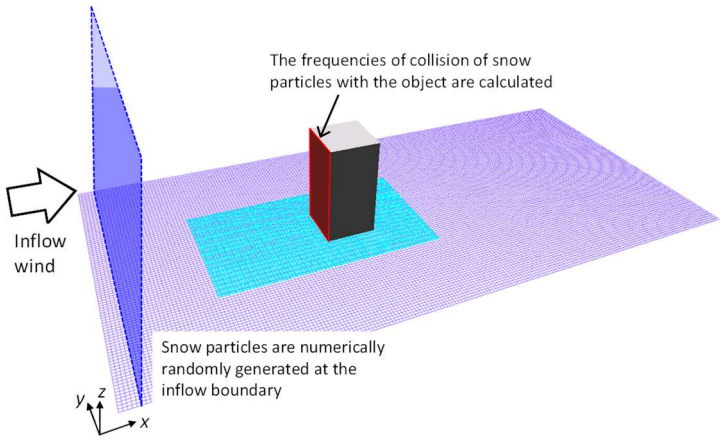

Figure 6. Computational domain (example of building size).

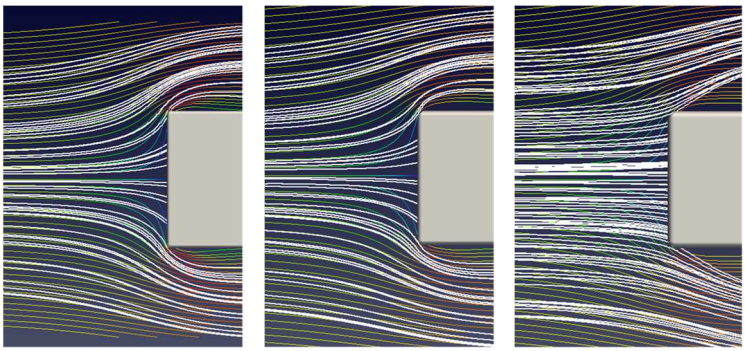

(1) W = 80 [m] (2) W = 10 [m] (3) W = 0.2 [m]

Figure 7. Trajectories of snow particles for horizontal section (z/H = 0.7). Thin lines: airflow streamlines, thick lines: Trajectories of snow particles.

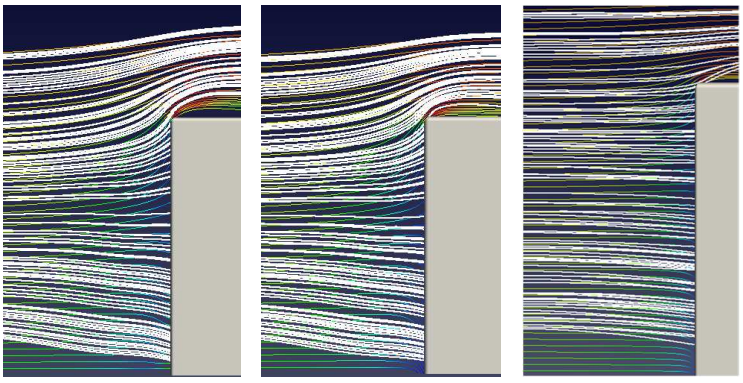

(1) W = 80 [m] (2) W = 10 [m] (3) W = 0.2 [m]

Figure 8. Trajectories of snow particles for vertical section (y/H = 0). Thin lines: airflow streamlines, thick lines: trajectories of snow particles.

of W = 80 m, it is found that many of the snow particles follow the airflow streamlines that change their direction in diverging ways in the area upwind of the object. This results in many of the snow particles avoiding collision with the central part of the object. A similar tendency was seen in the case of W = 10 min in Figure 7(2).

On the other hand, in the case of W = 0.2 m in Figure 7(3), snow particles collide rather uniformly with the object. This is because the airflow streamlines change direction in the upwind region close to the surface of the object to circumvent the obstacle, whereas snow particles are unable to change direction sufficiently to avoid collision owing to their inertia. Figure 8 shows a comparison of the streamlines of air flow and the trajectories of snow particles around objects in the vertical section at x/H = 0. In the cases of W = 80 m and W = 10 m in Figures 8(1) and (2), the snow particles move

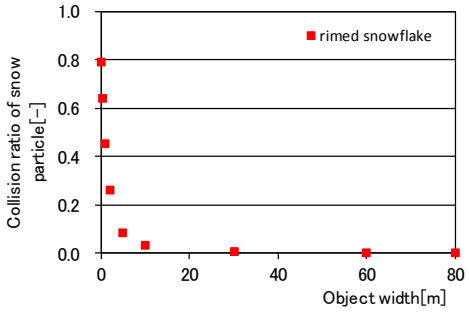

Figure 9. Relationships between object sizes and collision ratios.

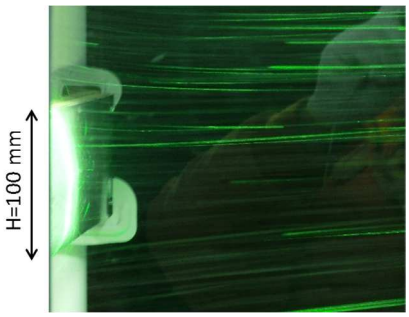

Figure 10. Visualization of snow particle collision.

almost along the airflow streamlines, and they are divided into the blow up and the down blow flows at a height of approximately z/H = 0.7. It is also found that the trajectories concentrate near the top edge of the object in the blow-up branch of the air flows. On the other hand, in the case of W = 0.2 m, the snow particles are again seen to travel straight to the object, as indicated by straight lines in the vertical section, and directly impinge the windward surface of the object.

The relationships between the collision ratios and the horizontal widths of the objects obtained by the simulations are shown in Figure 9. It is seen in the figure that the collision ratios have values of about 0.8 for W = 0.2 m, and they rapidly decrease with increases in object size and become far smaller than 0.1 for object widths that are larger than tens of meters. Figure 10 is an example of a visualization of snow particle collision with the test piece, which is a full-scale model of a member of the building material (Case 1) used in the wind tunnel experiments introduced in the previous sections.

The collision ratios obtained in the experiments were approximately 0.7–0.9. These values are rather well correspond to the ones obtained by numerical simulations (W = 0.2 m). Figure 11 shows density distribution of the points where snow particles collide with the wall of a building for projection widths of W = 80 m, 10 m, and 0.2 m. In the case of W = 80 m, a high-density range along the rim of the wall is clearly discernible. This feature of the collision density distribution is quite similar to the general tendency of snow adhesion distribution on building walls facing wind as observed in the outdoor surveys (Figure 1(2)).

Similar tendencies in the density distribution of collision points are also found in the case of W = 10 m, while the high density area, which was highly restricted near the rim of the building wall in the case of W = 80 m, extends farther to the central part of the building in this case. For W = 0.2 m, snow particles are seen to collide uniformly with the windward surface of the object. The collision ratio of about 0.8 for small objects (as shown in Figure 9) suggests that most of the incoming snow particles may directly impinge small objects, whereas only a small fraction of them collide with objects that have large projection widths.

These dependencies of the collision ratios on the size of the objects are commonly found both in the simulation and in the outdoor observations. They may result from the inertia of snow particles determining the degree of the deviation of the particle trajectories from the streamlines of the air flows around objects of different sizes. It is considered that the difference between the representative magnitudes of the curvatures and the stream lines of the flows among the objects of different sizes may be responsible for characterizing the types of snow adhesion.

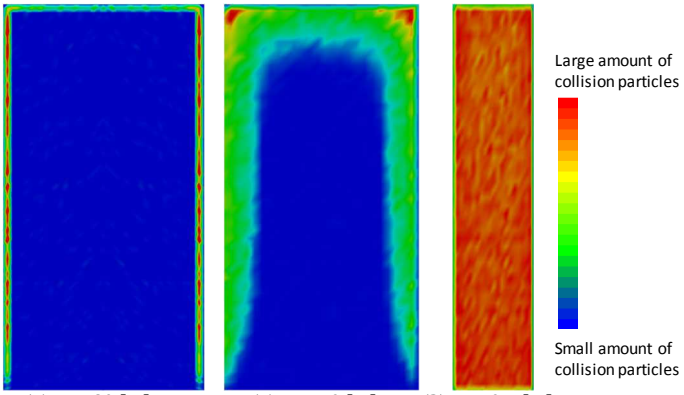

(1) D = 80 [m] (2) D = 10 [m] (3) D = 0.2 [m]

Figure 11. Distribution of particle collision density on building wall.

Conclusions

1) In order to investigate snow adhesion to objects having simple cross sections (flat plate), which are one type of object frequently used as building exterior (for example, vertical fins on a building wall), a series of wind tunnel experiments was carried out. It was found in the experiments that the cross sections of snow packs that adhered to the test pieces were generally windward facing and triangular. Peaks occurred along the center line of the object at a wind speed of 9 m/s, while a more rounded cross section was obtained at a wind speed of 5 m/s.

2) With regard to the snow adhesion having triangular cross sections, the rate of growth of the adhered snow pack by accretion was found to gradually decrease with time. This occurred because the stagnation region in front of the object simultaneously shrunk. This resulted from the increase in the degree of sharpness of the triangular cross section.

3) In order to examine the differences in snow accretion among objects of different sizes, CFD simulations using the Lagrangian particle method were carried out. The results obtained from the simulations were consistent with the differences in the way of snow accretion between small and large objects found in field observations.

4) It is suggested that the differences in the way of collision of snow particles between small and large objects resulted from the inertia effects of the mass of snow particles. This helps to characterize the dependencies in the way of snow accretion on the sizes of the objects.

References

[1] Tominaga, Y., Okaze, T. & Mochida, A., CFD Modeling of Snowdrift Around a Building: An Overview of Models and Evaluation of a New Approach, *Build Environ.*, **46**, 2011, 899–910.

[2] Beyers, M. & Waechter, B., Modeling Transient Snowdrift Development Around Complex Three-Dimensional Structures, *J. Wind Eng. Ind. Aerodyn.*, **96**, 2008, 1603–1615.

[3] Ishizaka, M., Measurement of Falling Velocity of Rimed Snowflakes, *Seppyo*, **57**, 229–238 (in Japanese).